AIP | Applied Physics Letters

Relaxation processes of point defects in vitreous silica from femtosecond to nanoseconds

A. Cannizzo, M. Leone, W. Gawelda, E. Portuondo-Campa, A. Callegari et al.

Citation: Appl. Phys. Lett. **93**, 102901 (2008); doi: 10.1063/1.2975965
View online: http://dx.doi.org/10.1063/1.2975965
View Table of Contents: http://apl.aip.org/resource/1/APPLAB/v93/i10
Published by the American Institute of Physics.

Related Articles

Coupling characteristics of point defects modes in two-dimensional magnonic crystals
J. Appl. Phys. 112, 103911 (2012)

A reaction diffusion model of pattern formation in clustering of adatoms on silicon surfaces
AIP Advances 2, 042101 (2012)

Convergent beam electron-diffraction investigation of lattice mismatch and static disorder in GaAs/GaAs1−xNx intercalated GaAs/GaAs1−xNx:H heterostructures
Appl. Phys. Lett. 101, 111912 (2012)

Response to “Comment on ‘Elastic wave propagation in a solid layer with laser-induced point defects’” [J. Appl. Phys. 112, 056101 (2012)]
J. Appl. Phys. 112, 056102 (2012)

Comment on “Elastic wave propagation in a solid layer with laser-induced point defects” [J. Appl. Phys. 110, 064906 (2011)]
J. Appl. Phys. 112, 056101 (2012)

Additional information on Appl. Phys. Lett.

Journal Homepage: http://apl.aip.org/
Journal Information: http://apl.aip.org/about/about_the_journal
Top downloads: http://apl.aip.org/features/most_downloaded
Information for Authors: http://apl.aip.org/authors

ADVERTISEMENT

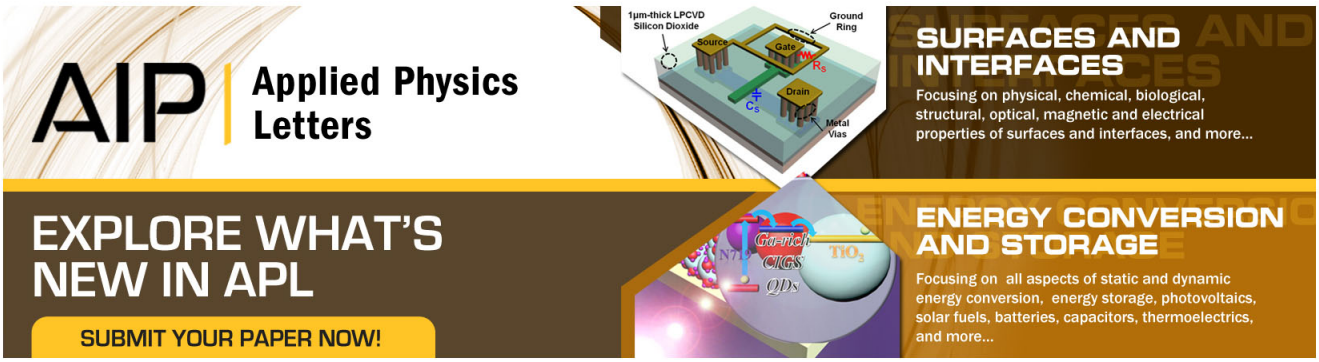

Relaxation processes of point defects in vitreous silica from femtosecond to nanoseconds

A. Cannizzo,[1,a)] M. Leone,[1] W. Gawelda,[2,b)] E. Portuondo-Campa,[2] A. Callegari,[2,c)] F. van Mourik,[2] and M. Chergui[2]
[1]*Dip. di Scienze Fisiche ed Astronomiche, Università di Palermo, Via Archirafi 36, I-90123 Palermo, Italy*
[2]*Ecole Polytechnique Fédérale de Lausanne, Laboratoire de Spectroscopie Ultrarapide, ISIC, CH-1015 Lausanne, Switzerland*

(Received 17 May 2008; accepted 1 August 2008; published online 8 September 2008)

We studied ultrafast relaxation of localized excited states at Ge-related oxygen deficient centers in silica using femtosecond transient-absorption spectroscopy. The relaxation dynamics exhibits a biexponential decay, which we ascribe to the departure from the Frank–Condon region of the first excited singlet state in 240 fs, followed by cooling in ~10 ps. At later times, a nonexponential relaxation spanning up to 40 ns occurs, which is fitted with an inhomogeneous distribution of nonradiative relaxation rates, following a chi-square distribution with one degree of freedom. This reveals several analogies with phenomena such as neutron reactions, quantum dot blinking, or intramolecular vibrational redistribution. © *2008 American Institute of Physics*.
[DOI: 10.1063/1.2975965]

Silica (amorphous SiO_2) is a material of paramount importance in solid-state physics and in material science[1] both because it provides a model for disordered amorphous systems and because of its widespread applications.[2] Many of these applications are related to optically active point defects, their generation (e.g., photosensitivity), and their relaxation dynamics upon excitation of localized excited states (e.g., in case of scintillators). During these processes, an excited defect and an out-of-equilibrium local matrix are created, which thermalize to a new configuration on the timescales of femtoseconds and picoseconds. There is a strong connection among the matrix dynamics on the subpicosecond timescale, photosensitivity, and point defect generation, as corroborated by studies on femtosecond laser-modified optical properties of silica[3] and by recent experimental and computational work.[4,5]

In this work, we used femtosecond transient absorption (TA) spectroscopy to identify the ultrafast relaxation processes of excited states localized on point defects in silica and their dynamical interaction with the local matrix. Specifically, we focus on Ge-related defects because of their fundamental role in photosensitivity and in optical device technology.[1] In particular the twofold coordinated Germanium (often indicated with $=Ge^{\cdot\cdot}$) has a distinct optical activity[6] (so-called B activity) and a rather simple energy level scheme, which makes it a suitable system for our studies. B activity consists of two broad (full width at half maximum ~0.5 eV) absorption bands at ~5 and at ~7.5 eV due to transitions from the $\boldsymbol{S_0}$ ground state to the first $\boldsymbol{S_1}$ and second $\boldsymbol{S_2}$ excited singlet states, respectively. Emission bands from $\boldsymbol{S_1}$ at ~4.2 eV and from the first excited triplet state $\boldsymbol{T_1}$ at ~3.1 eV have been observed, with typical room-temperature lifetimes of 2–4 ns and 110 μs, respectively.[6–9] The only nonradiative relaxation channel from $\boldsymbol{S_1}$ is a phonon-assisted intersystem crossing (ISC) to the $\boldsymbol{T_1}$ state, which occurs at $(\text{ns})^{-1}$ rates at room temperature.[6,8] Here, we follow in real time the conformational relaxation dynamics, upon excitation to the $\boldsymbol{S_1}$ state. The silica sample was doped with Ge atoms at $10^{-2}M$,[10] resulting in a final amount of $=Ge^{\cdot\cdot}$ of $\sim 10^{18}/\text{cm}^3$. As a reference, we have used an undoped, Ge free, commercial sample.[11] Both samples have optically polished surfaces and a nominal thickness of 1 mm.

TA measurements were performed in a pump-probe scheme. Femtosecond pump and probe pulses at 266 nm (4.7 eV) and 400 nm (3.1 eV), respectively, were obtained from the amplified output of a 1 kHz Ti:sapphire laser (nominally, 100 fs, 0.8 mJ, at 800 nm). Subsequently the two pulses were focused onto the sample with a spot size of ~70 μm for the pump and ~30 μm for the probe, orthogonally polarized with respect to each other. The cross correlation between the pump and probe pulses is 140 fs at the sample site. After verifying the linearity of the TA signal as a function of pump and probe intensities, these were set to 9×10^{12} and 3×10^{11} mW/cm^2 pulse, respectively. Under these conditions, we observe no significant bleaching of the optical B activity over several hours, as monitored by the intensity of the two emission bands induced by the pump pulse. Since the probe depletion ΔI was a small fraction of the transmitted probe intensity I_0, we calculated the TA signal as $\log_{10}(e)\cdot\Delta I/I_0$ as a function of time delay with respect to the pump pulse.

The TA kinetics of Ge-doped and undoped samples are shown in Fig. 1. The absence of any signal from the undoped specimen and the linear dependence of the probe depletion on the pump and probe intensity proves that the depletion signal is due to the B activity only, specifically to the $\boldsymbol{S_1}\rightarrow\boldsymbol{S_2}$ transition (see the aforesaid B-activity energy level scheme). Under our experimental conditions (linear regime and $\Delta I/I_0 \ll 1$), the signal is proportional to the product of the $\boldsymbol{S_1}$ population n_1 and the $\boldsymbol{S_1}\rightarrow\boldsymbol{S_2}$ absorption coefficient α, where in general both factors are time dependent. The

[a)]Present address: Ecole Polytechnique Fédérale de Lausanne (EPFL), LSU, ISIC, CH-1015 Lausanne, Switzerland. Electronic mail: andrea.cannizzo@epfl.ch.
[b)]Present address: Laser Processing Group, Instituto de Óptica, C.S.I.C., Serrano 121, E-28006 Madrid, Spain.
[c)]Present address: SICPA Management SA, Av. de Florissant 41, 1008 Prilly, Switzerland.

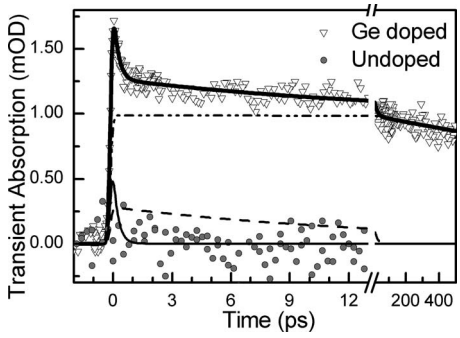

FIG. 1. TA as a function of pump-probe time delay for the Ge doped and undoped samples (triangles and circles, respectively). The total outcome (bold solid line) of fitting procedure in terms of the sum of two exponential decays and of a modified power-law (solid, dashed and double-point-dash lines, respectively) is reported [see Eqs. (1) and (2) and Table I].

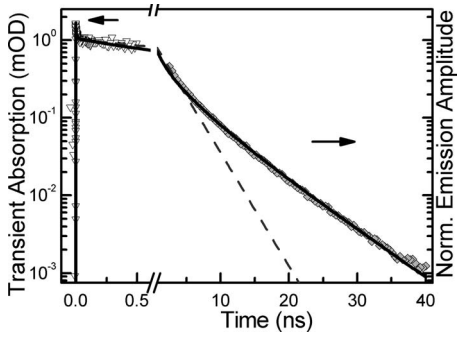

FIG. 2. Combination of time-resolved data from Fig. 1 (white triangles) with luminescence decay measurements from 2 to 40 ns (gray diamonds). Solid and dashed lines display the best fit using Eq. (1) and with a single exponential decay, respectively.

change of α is expected due to conformational rearrangement and cooling processes toward the S_1 energy minimum whereas n_1 is affected by the population loss from S_1 to S_0 and T_1. In Fig. 2, the TA kinetics of Fig. 1 is complemented with time resolved $S_1 \rightarrow S_0$ luminescence measurements from 2 up to 40 ns upon excitation at 4.7 eV previously reported (see Ref. 7). To merge them, we scaled the two data to match the expected $S_1 \rightarrow S_0$ emission quantum yield of 0.33.[12] Overall, we identify three main timescales: a fast exponential-like decay (<1 ps) followed by a slower one (~ 10 ps) and a third, nonexponential and much slower decay ($\sim$ns). We focus first on the early dynamics (≤ 20 ps). The two fast components are fitted with the sum of two exponential decays sitting on top of the slowest component. All these functions are convoluted with the temporal instrumental response which is assumed Gaussian

$$I(t) = \exp\left[-\tfrac{1}{2}(t/\sigma)^2\right] \otimes \left[I_P(t) + \sum_{i=1,2} I_i \cdot \exp(-t/\tau_i)\right], \quad (1)$$

where I_i and τ_i are amplitude and lifetime of the exponential decays, respectively, σ is the standard deviation of the instrumental response, and $I_P(t)$ accounts for the slowest component and just looks like a step function on this time scale [see Eq. (2) and relative discussion]. The fit and the relative parameters are reported in Fig. 1 and Table I, respectively.

The fastest processes occur on timescales typical of vibrations in silica (10^{-12}–10^{-13} s), and therefore we ascribe them to structural relaxation. This is in good agreement with recent computational results,[5] with the formation time of self-trapped excitons in bulk silica[13] and with the damping of vibrational modes related to four and three-membered SiO_2 ring structures.[4] This suggests that the shortest decay component corresponds to departure from the initial out-of-equilibrium configuration, mainly driven by the matrix dynamics. This result is supported by recent measurements, which have revealed that an isoelectronic substitution of Ge atoms with Sn atoms has a minor effect on the defect-matrix coupling.[14] The subsequent relaxation of the system on the ~ 10 ps timescale corresponds to vibrational cooling in the S_1 state, by dissipation to the matrix phonons.

We now turn to the slower decay kinetics (>20 ps). Based on the above discussion, the S_1 state is thermalized, and therefore the observed decay reflects its depopulation. The observed nonexponential decay of the $S_1 \rightarrow S_0$ luminescence signal (see data in Fig. 2 at $t > 2$ ns and compare them with dashed line in the same figure) has been related to an inhomogeneous dispersion of decay rates [specifically, of the nonradiative rates from S_1, since the radiative $S_1 \rightarrow S_0$ rate k_S $(1.28 \pm 0.03 \times 10^8\ \mathrm{s}^{-1})$ is not affected by inhomogeneous effects].[7,12] The data in the 20 ps–40 ns range of Fig. 2 are well described by the modified power law $I_P(t)$ (see solid line in Fig. 2 and Fig. 1 at time >20 ps),

$$I_P(t) = \frac{I_{\max} e^{-k_S t}}{(1 + \bar{k}_{\mathrm{ISC}} t)^{n/2}}, \quad (2)$$

where $\bar{k}_{\mathrm{ISC}}$ is a typical value for the $S_1 \rightarrow T_1$ ISC rate (see Table I for the parameter values). This law corresponds to the sum of individual exponential decays

$$\int_0^\infty e^{-(k_S + k_{\mathrm{ISC}})t} \chi^2_{n,\bar{k}_{\mathrm{ISC}}} dk_{\mathrm{ISC}}, \quad (3)$$

where the ISC rates k_{ISC} are dispersed according to a chi-square distribution $\chi^2_{n,\bar{k}_{\mathrm{ISC}}}$ with n degrees of freedom and $\bar{k}_{\mathrm{ISC}}$ as average value. Accordingly, $\bar{k}_{\mathrm{ISC}}$ agrees well with the rate which was estimated to $1 \times 10^9\ \mathrm{s}^{-1}$ from steady state luminescence measurements.[12] Remarkably, this distribution has been previously used to describe dynamical processes in many, seemingly unrelated systems, such as neutron reactions, quantum dot blinking, or intramolecular vibrational redistribution (see, e.g., Ref. 15). All these processes are found to be well described by random-matrix theory (RMT), which in general is suitable to describe chaotic and disordered systems, many-body quantum systems, and quantum localization.[15] A RMT description of our system is based on two assumptions on the spin-orbit Hamiltonian $\mathbf{H}^{\mathbf{SO}}$ coupling the initial state i (a vibrationally relaxed S_1 state, S_1^0) and N final states j (the hot vibrational states of T_1 resonantly coupled to S_1^0): (*i*) each individual defect corresponds to one of the possible realizations of $\mathbf{H}^{\mathrm{SO}}$, where the off-diagonal matrix elements H_{ij}^{SO} are well described as independently distributed around zero with Gaussian probability $P(H_{ij}^{\mathrm{SO}}) \propto \exp[-(H_{ij}^{\mathrm{SO}}/\bar{H}^{\mathrm{SO}})^2]$, with $\bar{H}^{\mathrm{SO}}$ being the average local coupling strength, (*ii*) the (inhomogeneous) ensemble of the defects probed corresponds to a large and statistically independent sample of all the possible random realizations of the spin-orbit Hamiltonian.

We recall that the ISC rate for a single defect is proportional to $\Sigma_j^N |H_{ij}^{\mathrm{SO}}|^2$, hence, if $\bar{H}^{\mathrm{SO}}$ is the same for every defect,

TABLE I. Amplitude I_{max}, time constant $\bar{k}_{ISC}^{-1}$ and exponent n for the power-law decay component and amplitudes $I_{1,2}$ and time constants $\tau_{1,2}$ for the biphasic exponential decay obtained from fitting the time domain data in Figs. 1 and 2 in terms of Eq. (1) and (2). The reported errors are twice the standard deviation.

Modified power law $I_P(t)$			
I_{Max} (arb. units)	$\bar{k}_{ISC}^{-1}$ (ns)	n	
0.0198 ± 0.0002	1.6 ± 0.2	1.00 ± 0.04	
Exponential decay			
I_1 (arb. units)	τ_1 (ps)	I_2 (arb. units)	τ_2 (ps)
0.018 ± 0.006	0.24 ± 0.09	0.0042 ± 0.0006	9.2 ± 1.6

the ensemble distribution of k_{ISC} is a χ^2 distribution with N degrees of freedom, and we should deduce that $N=1$, i.e., that $\boldsymbol{S_1^0}$ is coupled only to one vibrational level of $\boldsymbol{T_1}$. Yet this is typical for systems small enough that not all parts of the energetically allowed phase space are accessible and it can hardly be true for glassy systems. In this systems, excited states have a direct access to a high density of quantum states (see Ref. 15 and references therein for a more exhaustive discussion), that in our case are the vibrational states, related to the lattice local modes and coupled with the triplet state. On the other hand, if N is large, $\chi^2_{n,\bar{k}_{ISC}}$ looks like a narrowly peaked Gaussian, which is not compatible with the observed data. Indeed in the limit of $N \gg 1$, the distribution tends to a δ-function and $k_{ISC} \approx \bar{k}_{ISC} \propto |\bar{H}^{SO}|^2$, regardless of the chromophore. To reconcile this apparent contradiction, we have to go back to the assumption that $\bar{H}^{SO}$ and the H_{ij}^{SO} probability $P(H_{ij}^{SO})$ are the same for every defect. If this is straightforwardly the case of molecules in liquid solution or in gaseous phase where each explores all the possible configurations during the measurement process, it is not the case of defects in an amorphous solid (in this respect it is related to the ergodicity of the system). Therefore, still assuming that N is indeed large, $\bar{H}^{SO}$ is expected to be different for every defect and randomly distributed with a Gaussian probability centered on zero, which provide a one-degree χ^2 distribution for the ISC rates. In other words, the number of coupled states is high, but the dimensionality of the problem remains low, since the average coupling is modulated by some conformational coordinate. This hypothesis agrees with a recent model proposed to explain the thermal behavior of k_{ISC}. Authors describe the ISC process in terms of a $\boldsymbol{S_1} \rightarrow \boldsymbol{T_2} \rightarrow \boldsymbol{T_1}$ relaxation pathway, where the first step is governed by an activation barrier modulated by the O–Ge–O angle, while the second is barrier-less.[16] The main role of the O–Ge–O angle is also suggested by the strong localization of molecular orbitals involved in the electronic transition on the Ge atom.[17] Therefore we tentatively identify the O–Ge–O angle as the modulating coordinate, which shifts the energy position of $\boldsymbol{S_1}$ with respect to $\boldsymbol{T_2}$ because of the matrix local disorder. Since the $\boldsymbol{S_1}$-$\boldsymbol{T_2}$ barrier, which is <100 meV (~ 800 cm^{-1}), is of the same order of magnitude of the typical O–Ge–O bending vibration (~ 400 cm^{-1}),[18] a small variation in the crossing-point height will have a dramatic effect on the overlap of the $\boldsymbol{S_1^0}$ and $\boldsymbol{T_2}$ wave functions and, ultimately, on the coupling strength. Even if the number of hot states of $\boldsymbol{T_2}$ coupled with $\boldsymbol{S_1^0}$ is high, this near barrier-edge transition condition makes the coupling of $\boldsymbol{S_1^0}$ with the closest vibrational levels of $\boldsymbol{T_2}$ related to this mode critical for the ISC process, actually decreasing to one the number of effective channels.

In conclusion, we have investigated the photo-induced defect dynamics in silica over several decades from femtosecond up to tens of nanoseconds, and quantified the relaxation rates governing configurational changes and thermalization processes. Remarkably, we found that the dispersion of the ISC rates agrees with a χ^2 distribution with one degree of freedom. The quantitative characterization of relaxation rates can contribute to a deeper understanding of mechanisms for photosensitivity and defect generation and can provide important input for suitable theoretical models. Moreover, point defects in silica are an interesting clan of systems for studies of relaxation dynamics in solid amorphous matrices. On a more general perspective, the proposed idea of a strong decrease in the dimensionality of the process can provide an interpretation and analysis tool for numerous phenomena in amorphous systems, where a significant role of the lattice disorder has been observed but a satisfactory rationalization has not been found.

The authors would like to thank Professor R. Boscaino for useful discussions. A.C. is grateful to the ESF-ULTRA program for financial support. This work was supported by the Swiss NSF via Grant No. 2000-067912.02.

[1] R. A. B. Devine, J. P. Duraud, and E. Dooryhée, *Structure and Imperfections in Amorphous and Crystalline* SiO_2 (Wiley, Chichester, NY, 2000); G. Pacchioni, L. Skuja, and D. L. Griscom, *Defects in* SiO_2 *and Related Dielectrics : Science and Technology* (Kluwer, Dordrecht, 2000).
[2] S. R. Elliott, *Physics of Amorphous Materials*, 2nd ed. (Longman, New York/Wiley, New York, 1990); D. A. Keen and R. L. Mcgreevy, Nature **344**, 423 (1990); N. Mousseau, G. T. Barkema, and S. M. Nakhmanson, Philos. Mag. B **82**, 171 (2002); C. De Michele, P. Tartaglia, and F. Sciortino, J. Chem. Phys. **125**, 204710 (2006); G. N. Greaves and S. Sen, Adv. Phys. **56**, 1 (2007).
[3] K. Hirao and K. Miura, J. Non-Cryst. Solids **239**, 91 (1998).
[4] C. Guillon, J. Burgin, P. Langot, F. Vallee, and B. Hehlen, Appl. Phys. Lett. **86**, 081909 (2005).
[5] S. Sen and J. E. Dickinson, Phys. Rev. B **68**, 214204 (2003).
[6] L. Skuja, J. Non-Cryst. Solids **149**, 77 (1992).
[7] S. Agnello, R. Boscaino, M. Cannas, A. Cannizzo, F. M. Gelardi, S. Grandi, and M. Leone, Phys. Rev. B **68**, 165201 (2003).
[8] M. Leone, S. Agnello, R. Boscaino, M. Cannas, and F. M. Gelardi, in *Silicon-Based Materials and Devices*, edited by H. S. Nalwa (Academic, San Diego, 2001), Vol. 2, pp. 1–50.
[9] G. Pacchioni and R. Ferrario, Phys. Rev. B **58**, 6090 (1998).
[10] S. Grandi, P. Mustarelli, S. Agnello, M. Cannas, and A. Cannizzo, J. Sol-Gel Sci. Technol. **26**, 915 (2003).
[11] Shin-Etsu Quartz Products Co. Ltd., Suprasil-F300, Catalogue No. PC-FBR-SYN-001-E.
[12] A. Cannizzo, S. Agnello, R. Boscaino, M. Cannas, F. M. Gelardi, S. Grandi, and M. Leone, J. Phys. Chem. Solids **64**, 2437 (2003).
[13] S. Guizard, P. Martin, G. Petite, P. DOliveira, and P. Meynadier, J. Phys.: Condens. Matter **8**, 1281 (1996).
[14] A. Cannizzo, M. Leone, R. Boscaino, A. Paleari, N. Chiodini, S. Grandi, and P. Mustarelli, J. Non-Cryst. Solids **352**, 2082 (2006).
[15] T. A. Brody, J. Flores, J. B. French, P. A. Mello, A. Pandey, and S. S. M. Wong, Rev. Mod. Phys. **53**, 385 (1981); T. Uzer and W. H. Miller, Phys. Rep. **199**, 73 (1991); W. H. Miller, R. Hernandez, C. B. Moore, and W. F. Polik, J. Chem. Phys. **93**, 5657 (1990).
[16] A. Cannizzo, S. Agnello, S. Grandi, M. Leone, A. Magistris, and V. A. Radzig, J. Non-Cryst. Solids **351**, 1805 (2005).
[17] L. Skuja, J. Non-Cryst. Solids **239**, 16 (1998).
[18] F. L. Galeener, A. E. Geissberger, G. W. Ogar, and R. E. Loehman, Phys. Rev. B **28**, 4768 (1983).